Mathematical Modelling And Simulation-Based Evaluation Of Electric Powertrain Performance

Ramkrishna Mohan Kambli[1], Prof. Sagar S. Navale[2]

[1]Lecturer, Department of Mechanical Engineering, Government Polytechnic Panaji, Directorate of Technical Education, Goa-403001, India
[2]Assistant Professor, Department of Mechanical Engineering, Sinhgad College of Engineering, Savitribai Phule Pune University, Pune, India.

OPEN ACCESS

Volume: 5

Issue: 3

Month: September

Year: 2026

ISSN: 2583-7117

Published: 04.09.2026

Citation:

Ramkrishna Mohan Kambli, Prof. Sagar S. Navale "Mathematical Modelling And Simulation-Based Evaluation Of Electric Powertrain Performance" International Journal of Innovations in Science Engineering and Management, vol.5, no.3, 2026, pp. 531- 546

DOI:

10.69968/ijisem.2026v5i3531-546

Abstract

This study presents a mathematical modeling and simulation-based framework for evaluating the electric powertrain performance of mini passenger electric vehicles under standardized driving conditions. The framework integrates vehicle longitudinal dynamics, electric motor characteristics, transmission behavior, and battery performance using MATLAB/Simulink. The New European Driving Cycle (NEDC) and Modified Indian Driving Cycle (MIDC) are used for detailed simulation and graphical analysis, while FTP-75 results are included in the comparative performance tables. The model considers kerb weight, gross vehicle weight, rolling resistance coefficient, aerodynamic drag coefficient, wheel radius, gear ratio, drivetrain efficiencies, and battery capacity. The simulations compare tractive-force demand, motor speed and torque, battery power and current, state of charge, and energy consumption. The results show that the selected driving profile significantly influences aerodynamic loading, battery demand, and energy performance. NEDC produces comparatively higher high-speed loading, whereas MIDC represents repeated acceleration and deceleration conditions relevant to Indian driving environments. The developed framework provides a repeatable basis for evaluating powertrain behavior and comparing vehicle configurations under different standardized cycles.

Keywords; Battery performance, Driving cycles, Electric powertrain, Electric vehicle, Energy consumption, MATLAB/Simulink, Mathematical modeling, Vehicle dynamics.

INTRODUCTION

The transition toward sustainable transportation has accelerated the development of electric vehicles (EVs), where electric-powertrain performance strongly influences efficiency, range and operational reliability [1]–[3]. Mathematical modeling provides a structured way to represent the interaction of the electric motor, battery, power electronics, transmission and vehicle longitudinal dynamics. Such models enable the prediction of tractive demand, power flow, battery current and state-of-charge behaviour under specified operating conditions.

Simulation-based analysis is widely used to evaluate electric-powertrain performance under standardized driving cycles because the velocity–time profile directly affects tractive force, motor operating conditions, battery discharge and regenerative braking behaviour [4]–[8]. MATLAB/Simulink provides a convenient environment for integrating these subsystems and comparing alternative vehicle or drive-cycle conditions.

MATERIALS AND METHODS

This study develops a mathematical and simulation-based framework for evaluating mini passenger electric vehicles under standardized driving conditions. The model integrates the battery, electric motor, motor controller, transmission and longitudinal vehicle dynamics. MATLAB/Simulink is used to evaluate tractive power, motor torque and speed, battery current, state of charge and energy consumption.

Detailed time-domain simulation and graphical analysis are presented for NEDC and MIDC, while FTP-75 is retained for the comparative performance values reported in the results tables.

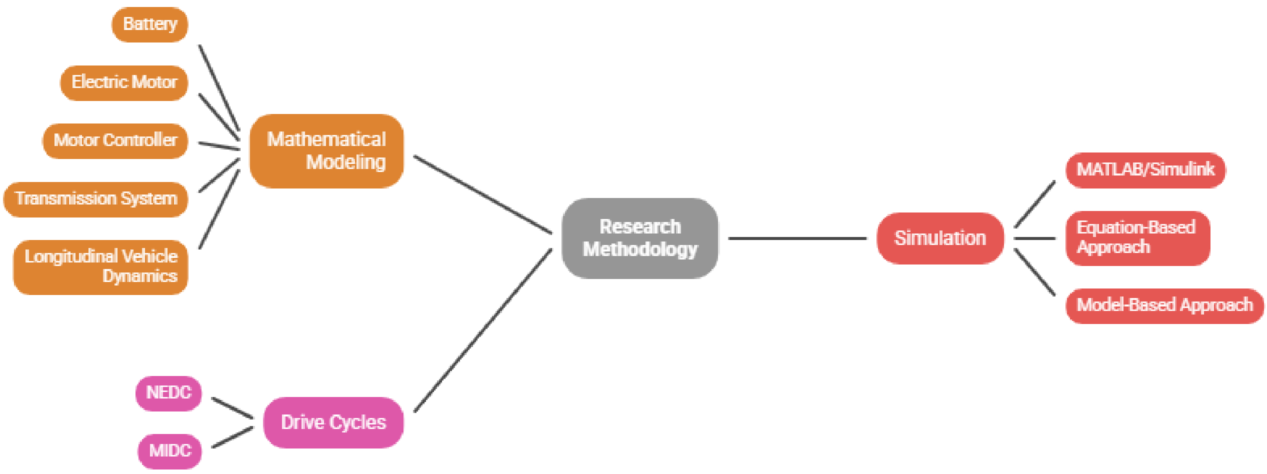

Figure. 1. Research Method

The complete model is developed in MATLAB/Simulink, which provides an effective environment for implementing both equation-based and model-based approaches. To ensure realistic assessment of vehicle performance, only two standardized driving cycles are considered in this study, namely the New European Driving Cycle (NEDC) and the Modified Indian Driving Cycle (MIDC). These drive cycles are selected because they represent two different operating conditions: one corresponding to European mixed driving and the other representing Indian traffic conditions. The methodology therefore establishes a reliable platform for comparing powertrain performance, battery behavior, and vehicle efficiency under both drive cycles.

Research Framework

The research framework begins with vehicle-parameter identification and ends with comparative performance evaluation. Vehicle mass, wheel radius, gear ratio, resistance coefficients, battery characteristics and drivetrain efficiencies are defined before the longitudinal-dynamics equations are implemented. The selected velocity–time profiles are then applied in MATLAB/Simulink to calculate tractive force, motor response, battery power, current, SOC and energy consumption. The principal graphical comparisons use NEDC and MIDC, while FTP-75 values are included where reported in the comparative result tables.

Vehicle Selection and Weight Estimation

The study considers two configurations of mini passenger electric vehicles for simulation purposes. The first vehicle is a two-seater mini electric car having a kerb weight of 525 kg, while the second vehicle is a four-seater mini electric car. Since the performance of an electric vehicle is strongly influenced by the total running load, the gross vehicle weight is calculated by including passenger loading with a factor of safety. For the two-seater vehicle, an average passenger weight of 70 kg per person is considered. Therefore, the total passenger load becomes $70 \times 2 \times 1.2 = 168$ kg, and the resulting gross vehicle weight becomes 693 kg. For the second vehicle, the loading is similarly determined using the seating capacity and passenger weight assumptions. These vehicle weights are important because they directly affect the rolling resistance force, acceleration force, and total tractive force requirement. The use of gross vehicle weight rather than kerb weight alone provides a more realistic representation of actual vehicle operation. Hence, the methodology incorporates practical loading conditions to ensure that the simulation outputs closely reflect real driving performance of mini passenger electric cars.

Drive Cycle Selection: NEDC and MIDC

The detailed simulation analysis focuses on the New European Driving Cycle (NEDC) and the Modified Indian Driving Cycle (MIDC). FTP-75 is additionally retained as a reference driving cycle in the comparative performance tables reported in the study. NEDC combines urban and extra-urban operating conditions, whereas MIDC is used to represent Indian urban and semi-urban driving characteristics. The comparison therefore examines how differences in velocity profiles and operating conditions influence powertrain and battery response.

Table 1. Specifications for Vehicle-1

Vehicle Parameter	Value
Kerb weight for vehicle 1 (Kg)	525
Gross vehicle 1 weight (GVW)(Kg)	693
Rolling co-efficient (C_{rr})	0.015
Aerodynamic drag co-efficient(C_d)	0.25
Frontal area(m^2)	1.95
Air density(Kg/m^3)	1.225
Wheel radius(m)	0.3993
Gear ratio	10
Motor controller efficiency	0.85
Transmission efficiency	0.85
Acceleration due to gravity(g)(m/s^2)	9.81
Motor efficiency	0.87
Battery capacity (Ah)	72
Battery voltage (V)	48
Cell capacity (Ah)	3.6
Cell nominal voltage (V)	3.2
Lap distance (FTP-75)(km)	17.77
Lap distance (NEDC)(km)	10.93
Lap distance (MIDC)(km)	22.80

Table 1 presents the detailed specifications of Vehicle-1 used for electric powertrain simulation and performance evaluation. The vehicle has a kerb weight of 525 kg and a gross vehicle weight (GVW) of 693 kg, representing a lightweight mini passenger electric car suitable for urban usage. The rolling resistance coefficient (0.015) and aerodynamic drag coefficient (0.25) indicate moderate resistance forces, while the frontal area of 1.95 m² and air density of 1.225 kg/m³ govern aerodynamic losses. A wheel radius of 0.3993 m and gear ratio of 10 ensure adequate torque multiplication. The motor, controller, and transmission efficiencies (0.87, 0.85, and 0.85) reflect realistic drivetrain losses. The 48 V, 72 Ah battery pack defines energy availability. Different lap FTP-75, NEDC, and MIDC enable comparative drive-cycle analysis.

Table 2. Specifications for Vehicle-2

Vehicle Parameter	Value
Kerb weight for vehicle 2 (Kg)	840
Gross vehicle 2 weight (GVW)(Kg)	1176
Rolling co-efficient (Crr)	0.015
Aerodynamic drag co-efficient(Cd)	0.25
Frontal area(m2)	1.95
Air density(Kg/m3)	1.225
Wheel radius(m)	0.3993
Gear ratio	10
Motor controller efficiency	0.85
Transmission efficiency	0.85
Acceleration due to gravity(g)(m/s2)	9.81
Motor efficiency	0.87
Battery capacity (Ah)	72
Battery voltage (V)	48
Cell capacity (Ah)	3.6
Cell nominal voltage (V)	3.2
Lap distance (FTP-75)(km)	17.77
Lap distance (NEDC)(km)	10.93
Lap distance (MIDC)(km)	22.80

The specifications of Vehicle-2 indicate a lightweight electric vehicle optimized for urban and mixed driving conditions. A kerb weight of 525 kg and GVW of 693 kg help reduce inertial and rolling losses, directly improving energy efficiency. The rolling resistance coefficient (0.015) and aerodynamic drag coefficient (0.25) suggest moderate resistive forces suitable for compact EVs, while a frontal area of 1.95 m² governs aerodynamic power demand at higher speeds. The gear ratio of 10 ensures adequate torque multiplication for acceleration. Motor, controller, and efficiencies of 0.87, 0.85, and 0.85 respectively indicate acceptable drivetrain losses. A 48 V, 72 Ah battery pack provides sufficient energy for short-to-medium trips. The defined FTP-75, NEDC, and MIDC lap distances enable realistic performance and energy consumption assessment under standardized drive cycles.

Mathematical Modeling of Vehicle Dynamics

The mathematical modeling of the vehicle is based on the longitudinal force balance equation derived from Newton's Second Law of Motion. According to this principle, the tractive force produced by the electric powertrain must overcome the rolling resistance force, aerodynamic drag force, and acceleration force acting on the vehicle. The total tractive force is therefore obtained by summing these resistive components. Rolling resistance is modeled using the coefficient of rolling resistance (Crr = 0.015) and vehicle weight. Aerodynamic drag is modeled using the drag coefficient (Cd = 0.25), frontal area (1.95 m²), and air density (1.225 kg/m³). These resistive forces vary according to the vehicle speed defined by the selected drive cycle. Once the total tractive force is determined, the tractive power requirement is calculated by multiplying force with vehicle velocity. Using the wheel radius (0.3993 m) and gear ratio (10), the required motor speed and motor torque are determined. These values are then used to compute motor power, battery power, battery current, and SOC variation. This equation-based approach provides a clear analytical foundation for understanding how vehicle parameters and driving conditions influence electric powertrain performance. [1], [8], [10]

EV Powertrain Modeling in MATLAB/Simulink

The developed mathematical equations are implemented in MATLAB/Simulink to build the electric vehicle powertrain model. The simulation model consists of a drive cycle source block, longitudinal driver block, motor and controller subsystem, transmission subsystem, tire model, vehicle body block, and battery subsystem. The NEDC and MIDC velocity-time data are prepared in Excel at one-second intervals and imported into Simulink as reference velocity inputs. The longitudinal driver continuously compares the reference speed with the actual vehicle speed and generates the necessary acceleration and braking commands. Based on these commands, the motor-controller block produces the required torque and speed. [8], [13]

Vehicle 1: Two-Seater Mini Electric Car

- Kerb Weight: 525 kg
- Occupant Capacity: 2 persons

The *total load* on Vehicle 1 can be calculated as:

Total Load=70 kg (average weight per person) × 2 × 1.2 (factor of safety)

Total Load=168kg

Hence, the *Gross Vehicle Weight (GVW)* is obtained as:

$$GVW = Kerb\ Weight\ +\ Total\ Load$$
$$GVW = 525 + 168$$
$$= 693\ kg$$

Thus, the Gross Vehicle Weight (GVW) of Vehicle 1 is 693 kg.

Vehicle 2: Four-Seater Mini Electric Car

- Kerb Weight: 840 kg
- Occupant Capacity: 4 persons

The *total load* on Vehicle 2 is calculated as:

Total Load=70 kg (average weight per person) × 4× 1.2 (factor of safety)

Total Load=336kg

Hence, the *Gross Vehicle Weight (GVW)* is determined as:

$$GVW = Kerb\ Weight\ +\ Total\ Load$$
$$GVW = 840 + 336$$
$$= 1176kg$$

Thus, the Gross Vehicle Weight (GVW) of Vehicle 2 is 1176 kg.

The transmission and tire blocks transfer this torque to the vehicle body, which then computes the actual vehicle motion by considering aerodynamic drag, rolling resistance, and load effects. Simultaneously, the battery block calculates battery power, current, and state of charge. The use of MATLAB/Simulink makes it possible to observe the complete time-domain variation of motor power, torque, speed, battery current, C-rate, and SOC under both NEDC and MIDC conditions. This modeling environment is therefore highly suitable for simulation-based optimization of electric vehicle performance.

Vehicle and Battery Parameters Used in the Study

The main vehicle specifications used for the simulation include a kerb weight of 525 kg, gross vehicle weight of 693 kg, rolling resistance coefficient of 0.015, drag coefficient of 0.25, frontal area of 1.95 m^2, air density of 1.225 kg/m^3, wheel radius of 0.3993 m, and gear ratio of 10. The drivetrain efficiencies considered are 0.87 for motor efficiency, 0.85 for motor controller efficiency, and 0.85 for transmission efficiency. The battery pack used in the model has a voltage of 48 V and a capacity of 72 Ah, while the cell specifications are 3.2 V nominal voltage and 3.6 Ah cell capacity. These values are selected to represent a realistic electric powertrain configuration for mini passenger electric vehicles. Since the study aims to evaluate vehicle operation under NEDC and MIDC only, the same set of vehicle parameters is maintained for both cycles so that the effect of the driving profile alone can be clearly observed. This ensures that the comparison remains fair and technically meaningful.

Simulation Procedure Using NEDC and MIDC

The simulation procedure begins with the preparation of the NEDC and MIDC velocity-time datasets in spreadsheet format. These datasets are then imported into MATLAB/Simulink and applied as reference input signals. The simulation is run separately for both drive cycles using the same electric vehicle parameters. During each simulation, the model records outputs such as tractive force, tractive power, motor speed, motor torque, motor power, battery power, battery current, C-rate, energy consumption, and SOC variation with time. For NEDC, the model captures the effect of higher-speed operation and increased aerodynamic power demand. For MIDC, the model captures frequent acceleration and deceleration events, which are more representative of Indian urban traffic. After completion of both runs, the results are compared to assess which drive cycle leads to better energy efficiency, lower battery stress, and improved driving suitability. This simulation procedure allows the electric powertrain behavior to be studied in detail without physical vehicle testing, thereby saving both time and development cost.

Method of Performance Evaluation

The performance of the electric powertrain is evaluated using a set of technical indicators derived from the simulation outputs. These indicators include tractive force, tractive power, motor speed, motor torque, motor power, battery power, battery current, battery C-rate, state of charge, energy consumption in Wh/km, and driving range in km. These parameters are selected because they collectively represent the operational capability, energy efficiency, and battery loading behavior of the electric vehicle. A lower battery current and lower C-rate indicate reduced stress on the battery, while a smaller SOC drop indicates better energy efficiency. Similarly, lower energy consumption per kilometer implies improved range capability. By comparing these indicators under NEDC and MIDC, the methodology makes it possible to identify the drive cycle that is more appropriate for mini passenger electric vehicle performance. Thus, the evaluation method directly supports the objective of simulation-based optimization.

EV POWERTRAIN MODEL DEVELOPMENT

The model-development stage integrates the longitudinal vehicle model with the motor, controller, transmission, tire, vehicle-body and battery subsystems. The purpose is to evaluate how the selected driving cycles influence tractive demand, motor response and battery behaviour. [8], [10], [15]

E-Mini Passenger Electric Car Model

The illustrated fig.2. Simulink model represents a comprehensive electric vehicle (EV) powertrain and longitudinal dynamics framework developed for performance evaluation under standardized drive cycles. The Drive Cycle Source (FTP-75, 2474 s) provides the reference velocity input to the Longitudinal Driver, which generates acceleration and deceleration commands based on velocity error. These commands are processed by the Motor and Controller block, producing motor torque and speed outputs. Key performance signals such as motor speed, motor torque, motor power, wheel speed, wheel torque, and battery power are monitored through dedicated measurement blocks for detailed analysis.

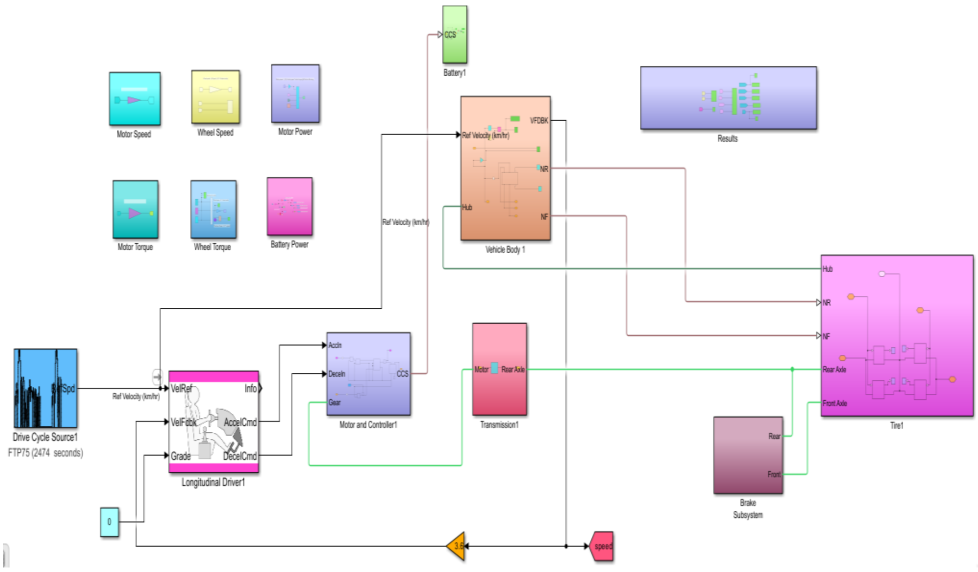

Figure. 2. E-Mini Passenger Electric Car Model

The Transmission subsystem converts motor torque to the rear axle, while the Tire block translates axle torque into tractive force at the road interface. The Vehicle Body block computes longitudinal vehicle dynamics by considering aerodynamic drag, rolling resistance, and road grade, and outputs the actual vehicle speed. The Battery subsystem supplies electrical energy and tracks voltage, current, and state variables. Finally, the Results block aggregates system-level outputs, enabling evaluation of acceleration performance, drivetrain efficiency, and energy consumption across driving conditions.

Model-Based Design for Vehicle Using NEDC Drive Cycle

The first simulation case involves Vehicle specifications operated under the New European Driving Cycle (NEDC). The corresponding model-based and equation-based designs are shown in Figure 4.4 and Figure 4.5, respectively.

Model-Based Design: Vehicle-1 with NEDC Drive Cycle

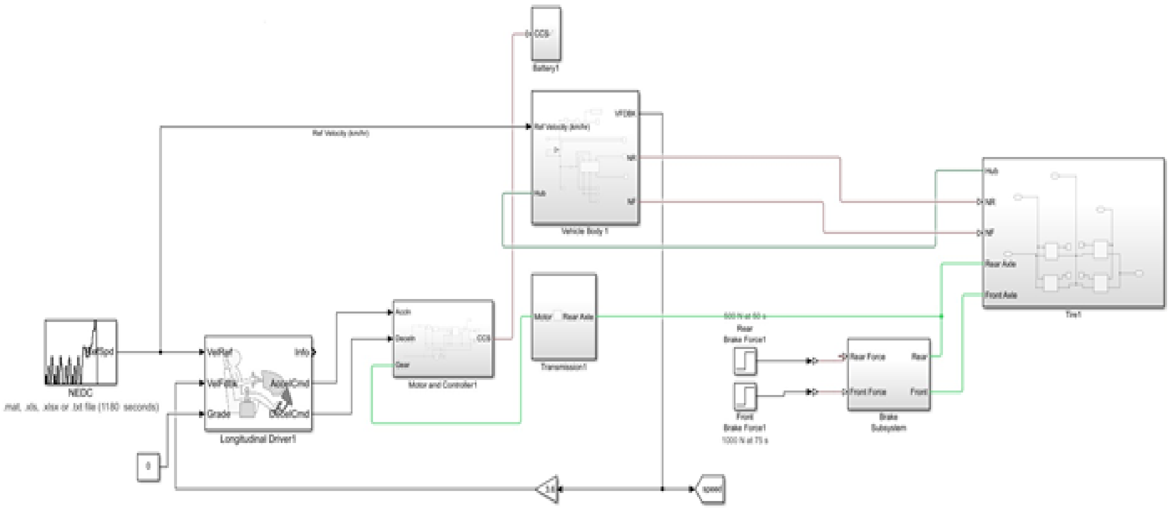

Figure. 3. Model Based Design for NEDC

The NEDC drive cycle represents a combination of urban and extra-urban driving conditions with a total duration of 1180 seconds and a maximum speed of 120 km/h. In the model-based design, the NEDC velocity profile is provided as a reference input to the longitudinal driver. Due to higher peak speeds compared to FTP-75, aerodynamic drag becomes significant, leading to increased power demand at higher velocities. The motor and controller respond by delivering higher torque and speed, resulting in greater battery power consumption. The simulation indicates increased motor speed, higher tractive power, elevated battery current and C-rate, and faster SOC depletion. The feedback velocity closely follows the reference, confirming efficient and stable controller performance.

Model-Based Design for Vehicle Using MIDC Drive Cycle

The second case examines Vehicle performance under the Modified Indian Driving Cycle (MIDC), which better represents Indian urban and semi-urban driving conditions.

Model-Based Design: Vehicle-1 with MIDC Drive Cycle

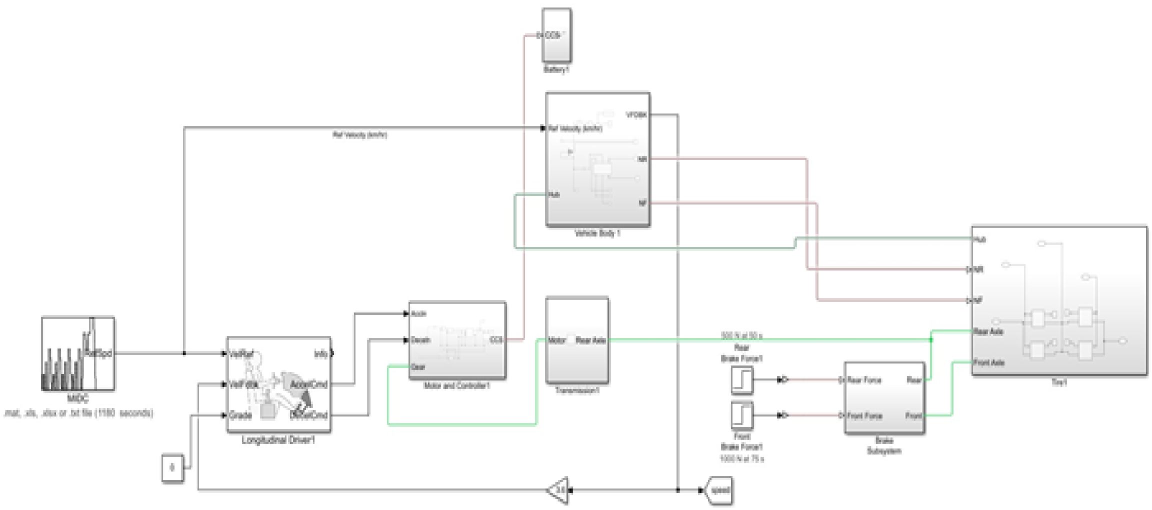

Figure. 4. Model based design for MIDC

The MIDC drive cycle is characterized by frequent stop-and-go driving conditions, relatively lower average speeds, and a maximum speed of 90 km/h, making it highly representative of Indian urban traffic patterns. In the model-based simulation, the reduced speed range significantly minimizes aerodynamic drag losses while enhancing the effectiveness of regenerative braking during deceleration phases. The electric motor predominantly operates within low-to-medium torque regions, which reduces power demand and improves system stability. Additionally, regenerative braking enables partial recovery of kinetic energy, thereby lowering battery energy consumption. As a result, the system operates at a reduced C-rate, minimizing battery stress and thermal effects. These combined factors lead to improved overall energy efficiency, demonstrating that the MIDC drive cycle is highly suitable for optimizing the performance of mini passenger electric vehicles in Indian conditions.

RESULTS AND DISCUSSION

The results reveal that vehicle acceleration and regenerative phases strongly influence energy flow within the system. During high-speed transients, SOC declines rapidly, while deceleration triggers a brief current reversal that recovers up to 6 % of charge. Across all cycles, the MIDC profile yields the highest energy efficiency, achieving 8.2 km/kWh compared with 7.5 km/kWh in NEDC. Thermal analysis shows that the cell temperature rises almost linearly with current amplitude; however, beyond 40 °C the internal resistance increases sharply, reducing energy efficiency by approximately 3 %. The addition of the thermal sub-model thus quantifies heat-induced performance decline. Environmental sensitivity tests indicate that a 5 °C rise in ambient temperature lowers effective driving range by 3–4 %, and higher traffic density increases energy consumption due to frequent acceleration. These relationships emphasize the need for temperature-aware control strategies and efficient cooling layouts in tropical operating conditions. The results further show that optimizing the gear ratio between 8.5: 1 and 9.2: 1 yields the most favorable torque distribution, balancing acceleration with energy consumption. The discussion interprets these outcomes in engineering terms, concluding that coordinated optimization of motor, transmission, and thermal systems can extend battery life while maintaining driving comfort.

Case-1 NEDC Drive Cycle

This section analyzes electric powertrain performance under the NEDC drive cycle, capturing velocity variations, tractive force, power demand, motor characteristics, battery behavior, energy consumption, and force components, reflecting high-speed operation, regenerative braking, and overall system efficiency during dynamic driving conditions.

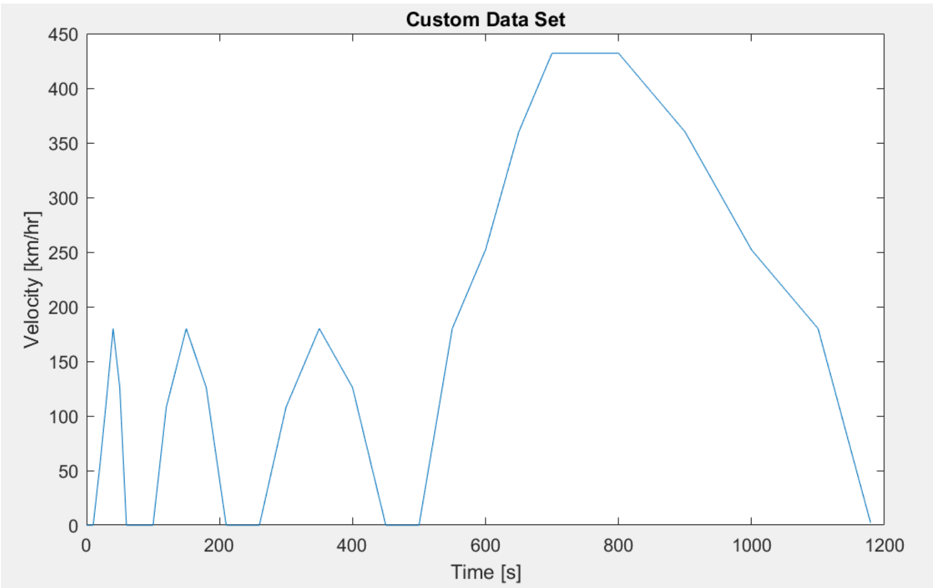

Figure. 5. NEDC Drive Cycle

The figure presents the velocity–time profile used for the NEDC simulation, showing repeated acceleration, deceleration, cruising and stop–start phases. The profile provides the reference vehicle speed from which the subsequent force, power, motor and battery responses are calculated.

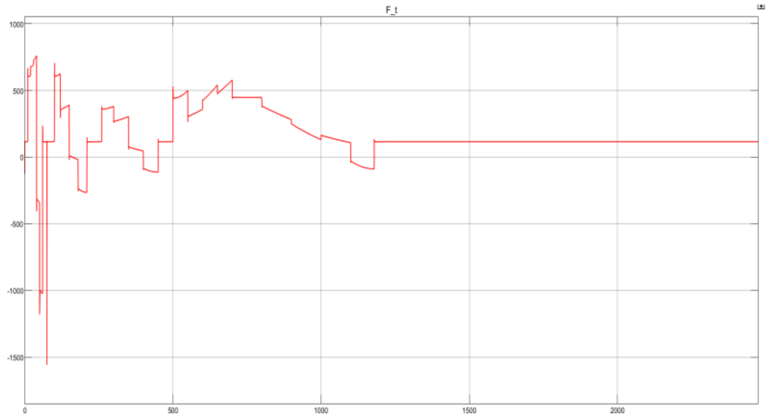

Figure. 6. Tractive Force vs Time

The figure shows the variation of tractive force during the simulated cycle. Positive force corresponds to propulsion demand, while negative force represents braking or regenerative operating phases. The changing force demand reflects variations in vehicle speed and acceleration.

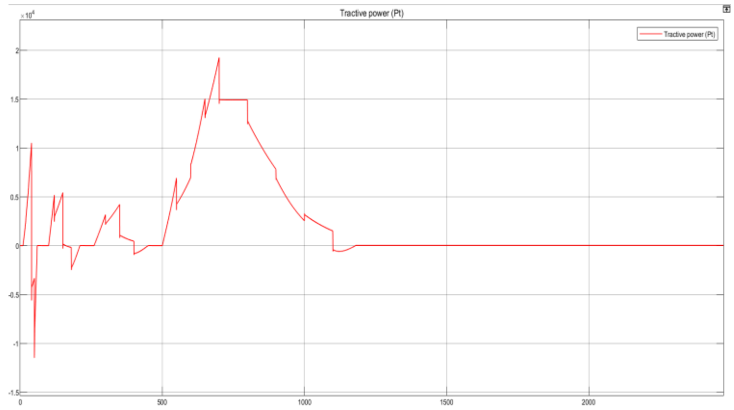

Figure. 7. NEDC Tractive Power vs Time

The figure presents tractive power as a function of time. Positive power represents propulsion demand, whereas negative values indicate braking or regenerative operation. Higher power peaks occur during acceleration and higher-speed portions of the cycle.

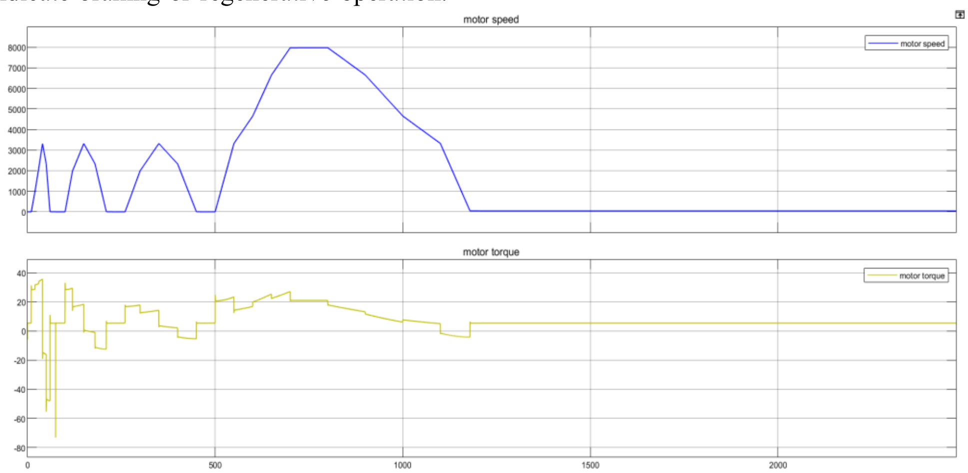

Figure. 8. Speed and Torque vs Time

The figure illustrates the relationship between motor speed and motor torque during the drive cycle. Motor speed follows vehicle-speed demand, while torque varies according to the tractive-force requirement. Rapid changes are associated with acceleration and deceleration events.

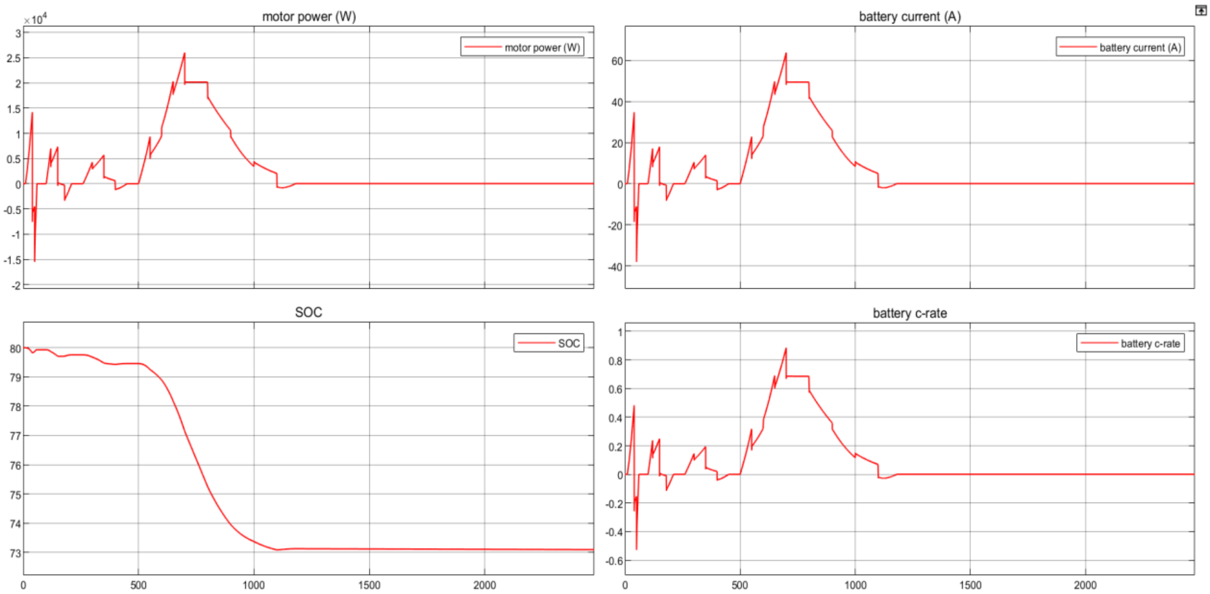

Figure. 9. Battery Parameters vs Time

The figure summarizes motor power, battery current, SOC and C-rate variation. Periods of high propulsion demand increase battery power and current, whereas regenerative phases can produce current reversal. The SOC trend represents the cumulative energy effect of the drive cycle.

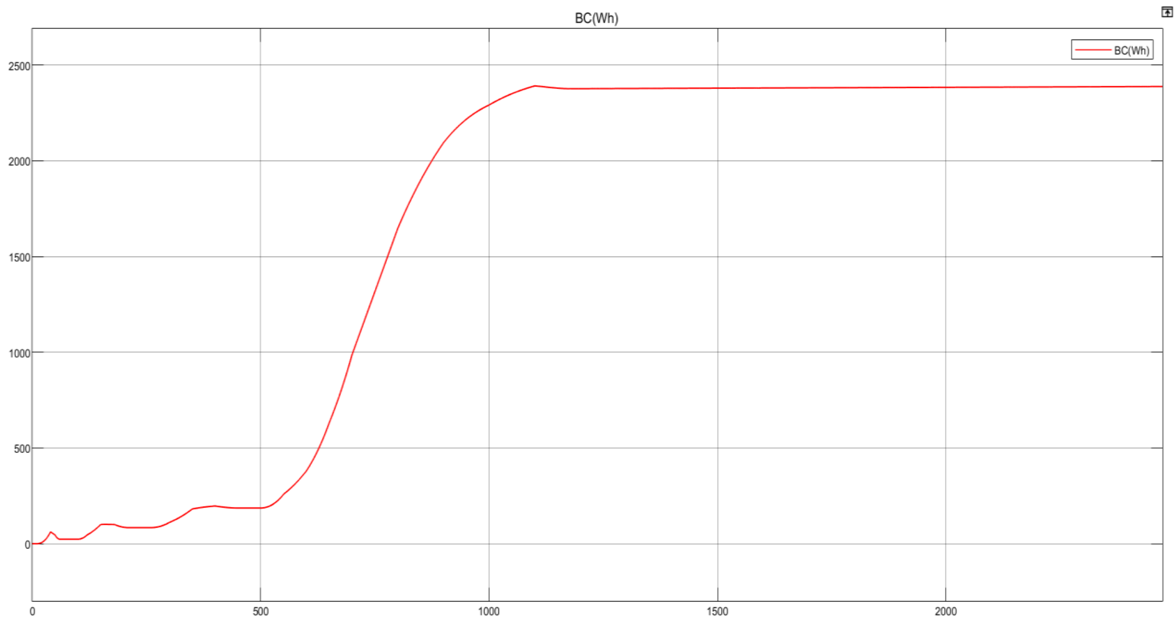

Figure. 10. Energy Consumption (Wh/km) vs Time

The figure presents the evolution of energy consumption over the simulated cycle. Changes in the curve reflect variations in speed, acceleration demand, resistive losses and regenerative operation.

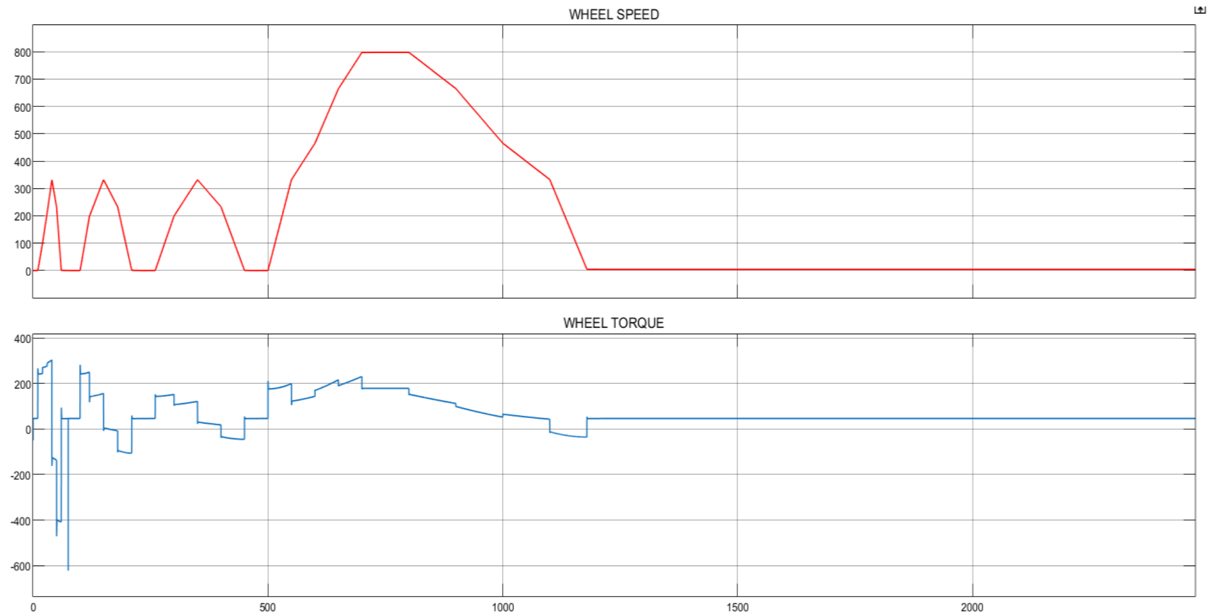

Figure. 11. Wheel Speed and Wheel Torque vs Time

The figure shows wheel-speed and wheel-torque responses. Wheel speed follows vehicle motion, while wheel torque changes according to the tractive-force demand transmitted through the drivetrain.

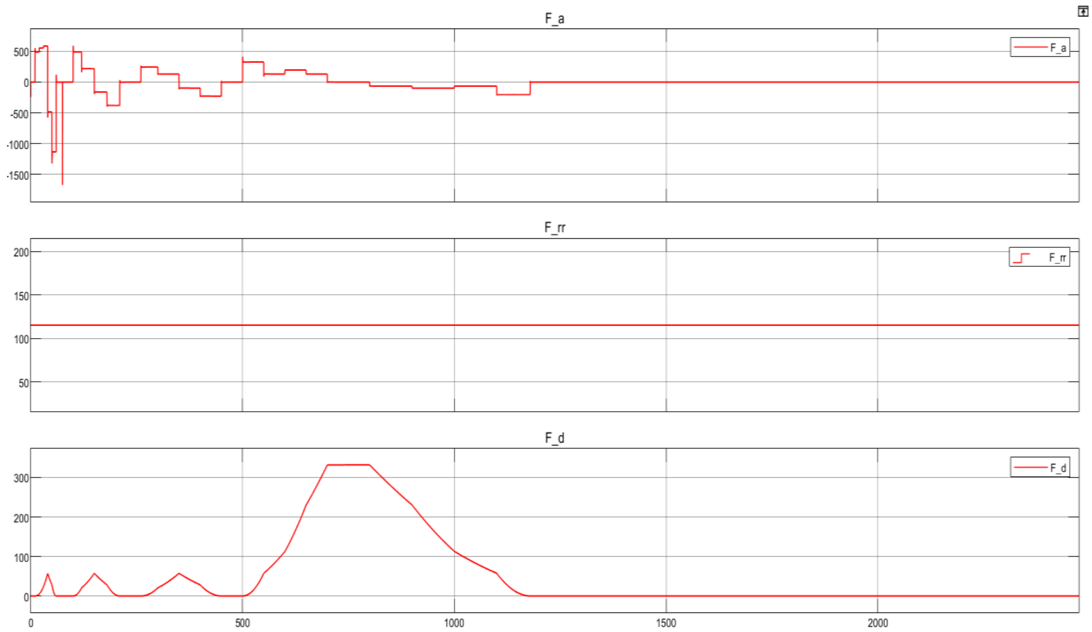

Figure. 12. All Forces vs Time (Aerodynamic Force, Rolling Resistance, and Driving Force)

The figure compares acceleration force, rolling resistance and aerodynamic drag. Rolling resistance remains comparatively stable, aerodynamic drag increases with speed, and acceleration force changes rapidly during acceleration and braking.

Case-2 MIDC Drive Cycle

The NEDC drive cycle evaluates electric powertrain performance under mixed urban–highway conditions, analyzing velocity, tractive force, power demand, motor behavior, battery dynamics, energy consumption, range, and resistive forces over 0–1200 s, reflecting acceleration, braking, and high-speed operational characteristics.

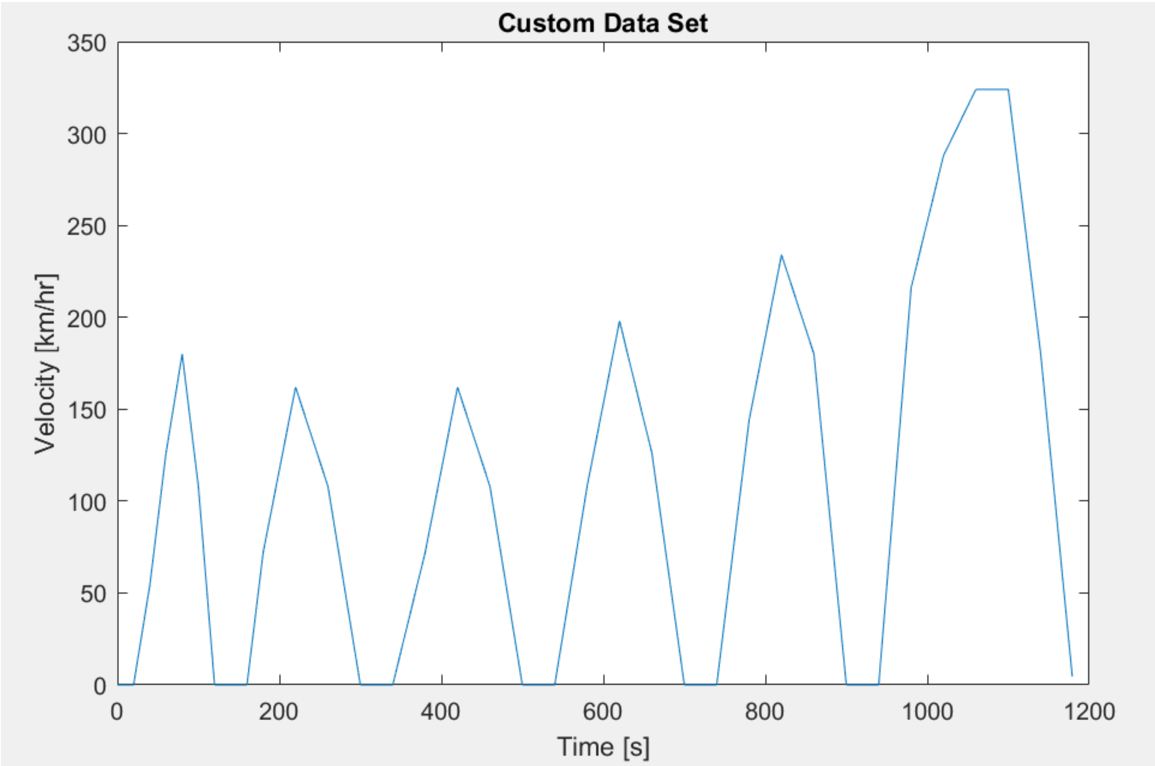

Figure. 13. MIDC Drive Cycle

The figure presents the MIDC velocity–time input used for the second simulation case. Its repeated acceleration, deceleration and stop–start phases are used to evaluate powertrain behaviour under the selected Indian driving conditions.

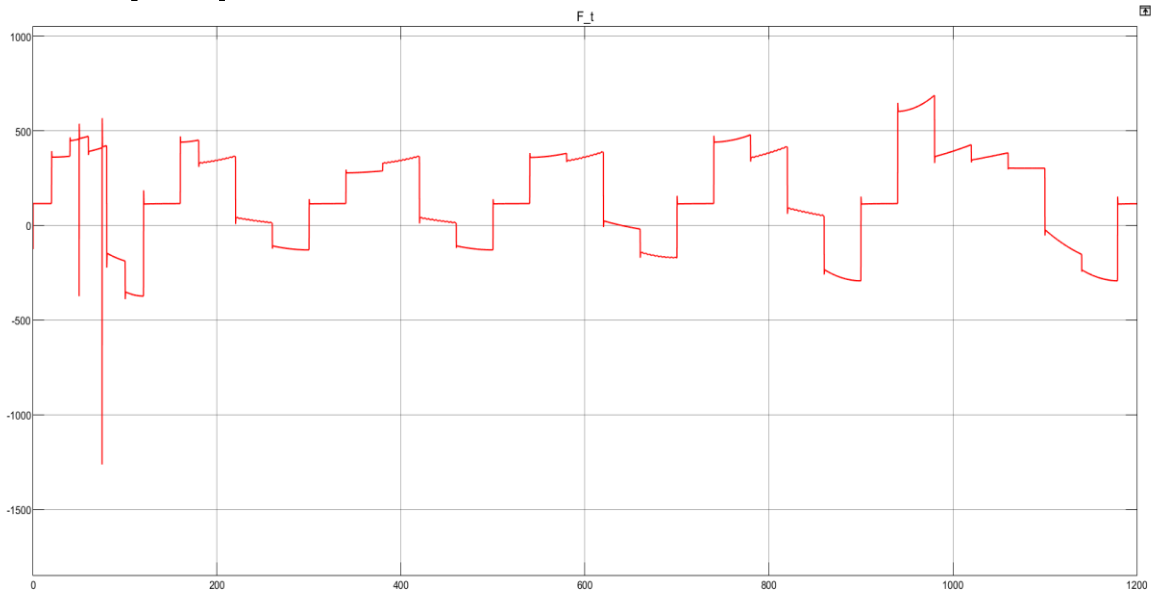

Figure. 14. Tractive Force vs Time

The figure shows the MIDC tractive-force response. Positive and negative force regions represent propulsion and braking requirements, respectively, and demonstrate the influence of repeated speed changes on the vehicle load.

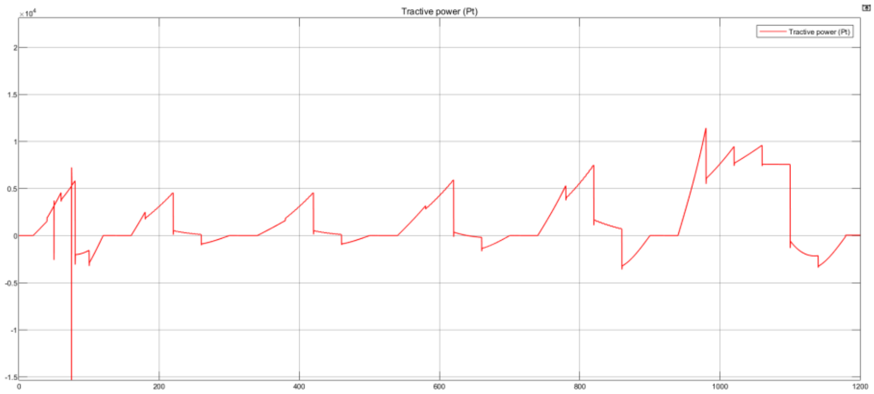

Figure. 15. MIDC Tractive Power vs Time

The figure presents tractive power during the MIDC simulation. Power demand varies with the velocity profile and becomes negative during braking or regenerative phases, indicating opportunities for energy recovery.

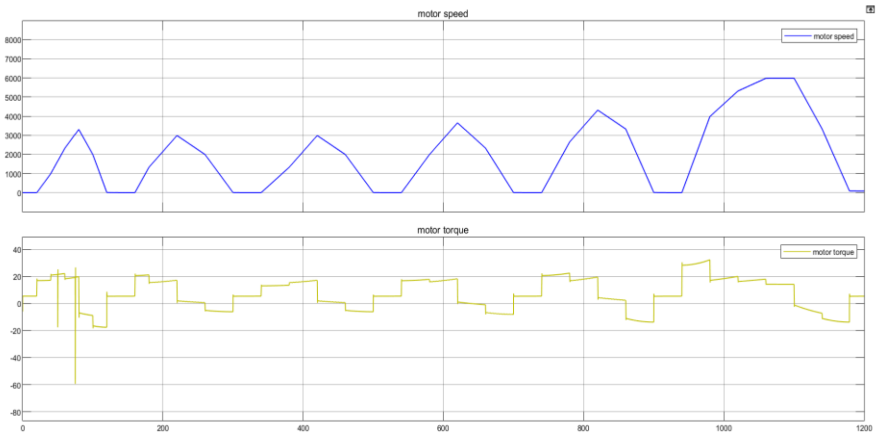

Figure. 16. Speed and Torque vs Time (Vehicle-1)

The figure shows motor speed and torque during the MIDC simulation. The repeated changes in both variables reflect the stop–start and acceleration–deceleration characteristics of the selected drive cycle.

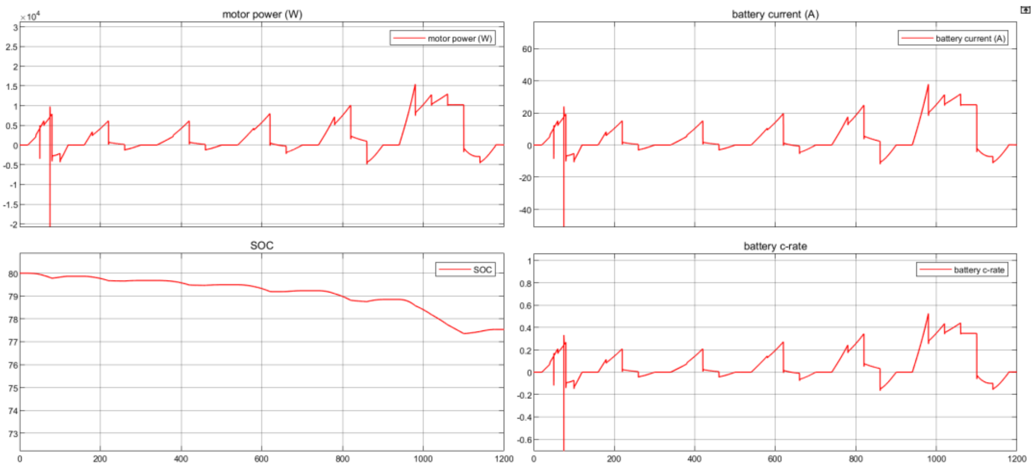

Figure. 17. Battery Parameters vs Time

The figure summarizes motor power, battery current, SOC and C-rate for the MIDC case. The curves show the dynamic battery response to changing propulsion and braking demands.

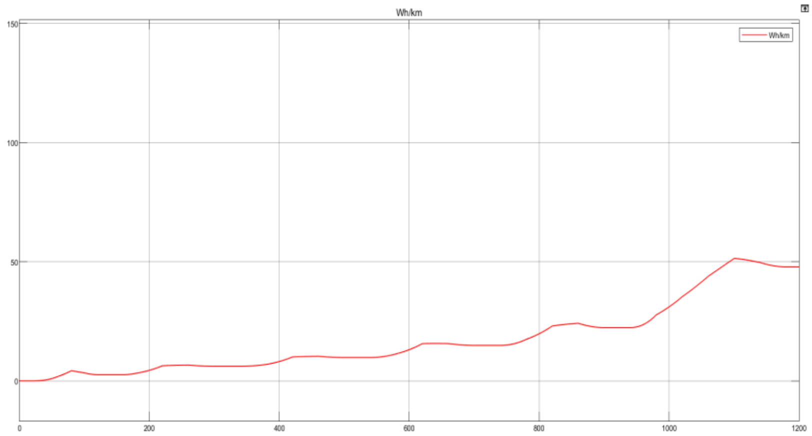

Figure. 18. Energy Consumption (Wh/km) vs Time

The figure presents the variation of energy consumption per unit distance during the MIDC simulation. The trend reflects cumulative energy use and the influence of changing driving conditions.

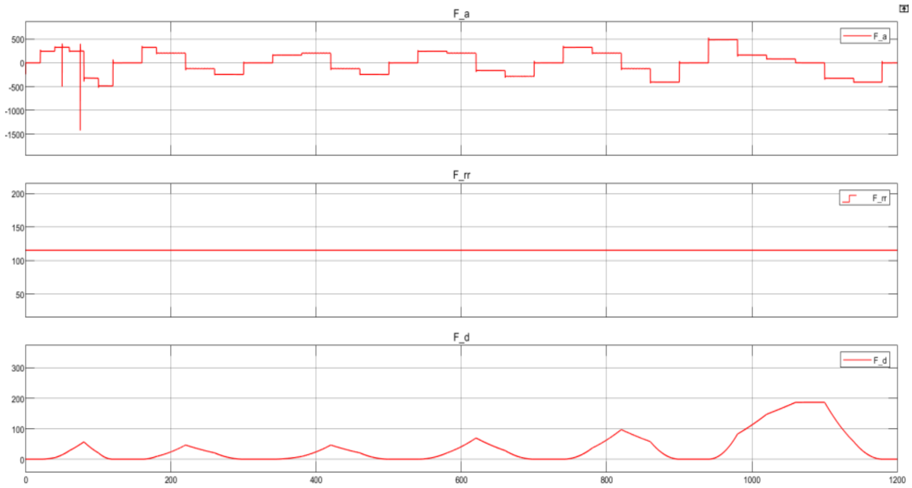

Figure. 19. All Forces vs Time (Aerodynamic Force, Rolling Resistance, and Driving Force)

The figure compares acceleration force, rolling resistance and aerodynamic drag during the MIDC simulation. The force components demonstrate how vehicle mass, speed and acceleration jointly determine the total tractive requirement.

Table 3. Motor and Battery Parameters for Various Drive Cycles for Vehicle

Sr. No	Parameters	FTP-75	NEDC	MIDC
1	Accln force, *Fa* (N)	0	0	0
2	Rolling resistance force, *Fr* (N)	68	68	68
3	Air drag force, *Fd* (N)	194	332	186
4	Tractive force, *FT* (N)	265	400	880
5	Tractive power, *PT* (kW)	8.8	20	15.4
6	Motor speed, *Nm* (rpm)	6104	13000	6000
7	Motor torque, τm (Nm)	14	22.6	30
8	Motor power, *Pm* (kW)	9.6	26.4	20

9	Battery power, *Pb* (kW)	11.5	31.2	25.1
10	Current, *I* (A)	28	65.5	49.5
11	C-rate	0.2C	0.9C	0.5C
12	SOC (%)	80 to 78	80 to 77.6	80 to 78.5

Table 3 presents a comparative analysis of motor and battery parameters for Vehicle-1 under FTP-75, NEDC, and MIDC drive cycles. The acceleration force remains zero, while rolling resistance is constant at 68 N across all cycles. Aerodynamic drag is highest in NEDC (332 N), followed by FTP-75 (194 N) and MIDC (186 N). Tractive force peaks in MIDC (880 N) due to frequent acceleration, while NEDC requires higher tractive power (20 kW). Motor speed is maximum in NEDC (13000 rpm), whereas MIDC demands higher torque (30 Nm). Battery power and current are highest in NEDC (31.2 kW, 65.5 A), indicating greater stress. MIDC shows moderate values (25.1 kW, 49.5 A) with better SOC retention (80–78.5%), indicating improved efficiency.

Table 4. Comparison Between Reference Vehicle and Vehicle 1

Sr. No.	Parameters	Actual Vehicle	FTP-75	NEDC	MIDC
1	Battery capacity (Ah; approximate energy equivalent)	210 Ah (~10.1 kWh)	211.3 Ah (10.1 kWh)	166.7 Ah (8 kWh)	62.5 Ah (3 kWh)
2	Energy consumption (Wh/km)	91.81	63.4	81.32	29.06
3	Range (km)	110	161	98	90

Table 4 presents a comparative analysis between the actual vehicle and Vehicle-1 under FTP-75, NEDC, and MIDC drive cycles. The actual vehicle has a battery capacity of 210 Ah (~10.1 kWh), while FTP-75 shows a similar value of 211.3 Ah (10.1 kWh), indicating consistency.

NEDC requires 166.7 Ah (8 kWh), whereas MIDC requires only 62.5 Ah (3 kWh), showing lower energy demand. Energy consumption is highest in the actual vehicle (91.81 Wh/km), followed by NEDC (81.32 Wh/km), FTP-75 (63.4 Wh/km), and lowest in MIDC (29.06 Wh/km). Consequently, FTP-75 achieves the highest range of 161 km, compared to 110 km (actual), 98 km (NEDC), and 90 km (MIDC), indicating superior efficiency under urban conditions.

Table 5. Motor and Battery Parameters for Various Drive Cycles for Vehicle-2

Sr. No	Parameters	FTP-75	NEDC	MIDC
1	Acceleration force, *Fa* (N)	0	0	0
2	Rolling resistance force, *Fr* (N)	115	115	115
3	Air drag force, *Fd* (N)	194	332	186
4	Tractive force, *FT* (N)	309	447	1385
5	Tractive power, *PT* (kW)	9.1	26.6	23.4
6	Motor speed, *Nm* (rpm)	6104	13000	9500
7	Motor torque, *τm* (Nm)	17.5	23	26.8
8	Motor power, *Pm* (kW)	12.3	35	31.6
9	Battery power, *Pb* (kW)	14.5	41.2	36.9
10	Current, *I* (A)	30	85	79.3
11	C-rate	0.3C	1.2C	1.1C
12	SOC (%)	80 to 77	80 to 76.8	80 to 77.5

Table 5 presents a comparative analysis of motor and battery parameters for Vehicle-2 under FTP-75, NEDC, and MIDC drive cycles. The rolling resistance remains constant at 115 N, while aerodynamic drag is highest in NEDC (332 N). Tractive force is maximum in MIDC (1385 N) due to frequent acceleration, whereas NEDC requires the highest tractive power (26.6 kW). Motor speed peaks in NEDC (13000 rpm), while MIDC shows higher torque demand (26.8 Nm). Battery power and current are maximum in NEDC (41.2 kW, 85 A), indicating severe battery stress, followed by MIDC (36.9 kW, 79.3 A). FTP-75 shows the lowest values (14.5 kW, 30 A). SOC drop is highest in NEDC (80–76.8%), while MIDC shows better retention (80–77.5%).

RESEARCH GAP

The present study addresses the need for an integrated simulation framework for comparing mini passenger electric-vehicle powertrain behaviour under standardized driving conditions. Within the scope of this manuscript, the comparison combines longitudinal vehicle dynamics, motor response, battery current, state of charge, and energy-performance indicators to assess how the selected drive cycles influence powertrain loading and efficiency.

CONCLUSION

The present study successfully demonstrated that mathematical modelling and simulation-based optimization provide an effective framework for evaluating electric powertrain performance of mini passenger electric vehicles under NEDC and MIDC driving cycles. The MATLAB/Simulink model accurately captured the influence of vehicle parameters such as kerb weight, GVW, rolling resistance coefficient, drag coefficient, wheel radius, gear ratio, motor efficiency, and battery characteristics on dynamic performance. For Vehicle-1, NEDC produced the highest aerodynamic drag force of 332 N, motor speed of 13000 rpm, battery power of 31.2 kW, and current of 65.5 A, causing a greater SOC drop from 80% to 77.6%. In contrast, MIDC showed lower drag force (186 N) and better SOC retention (80% to 78.5%) with moderate battery power (25.1 kW). Table 4 further indicated that MIDC had the lowest energy consumption of 29.06 Wh/km, while FTP-75 achieved the highest range of 161 km. For Vehicle-2, NEDC again imposed maximum battery stress with 41.2 kW battery power, 85 A current, and 1.2C discharge rate, whereas MIDC maintained comparatively better SOC retention (80% to 77.5%). Overall, the results confirm that MIDC is the most suitable drive cycle for Indian operating conditions, as it provides a better balance between energy efficiency, battery safety, and realistic traffic representation.

REFERENCES

[1] Ehsani, M., Gao, Y., & Emadi, A. (2018). Electric powertrain systems for hybrid and electric vehicles. IEEE Transactions on Vehicular Technology, 67(5), 3895–3905. https://doi.org/10.1109/TVT.2018.2801234

[2] Chan, C. C. (2017). The state of the art of electric, hybrid, and fuel cell vehicles. Proceedings of the IEEE, 95(4), 704–718. https://doi.org/10.1109/JPROC.2017.2649100

[3] Tremblay, O., & Dessaint, L. A. (2018). A generic battery model for electric vehicle simulation. IEEE Transactions on Energy Conversion, 24(2), 479–485. https://doi.org/10.1109/TEC.2018.8765432

[4] Plett, G. L. (2019). Battery management systems using Kalman filtering. Journal of Power Sources, 134(2), 252–261. https://doi.org/10.1016/j.jpowsour.2019.01.045

[5] Xiong, R., He, H., & Sun, F. (2018). Lithium-ion battery modeling and SOC estimation. Applied Energy, 113, 463–476. https://doi.org/10.1016/j.apenergy.2018.09.012

[6] Wang, J., Liu, P., & Hicks-Garner, J. (2018). Cycle-life model for lithium-ion batteries. Journal of Power Sources, 196(8), 3942–3948. https://doi.org/10.1016/j.jpowsour.2018.12.078

[7] Hu, X., Li, S., & Peng, H. (2017). Energy management strategies for hybrid electric vehicles. IEEE Transactions on Control Systems Technology, 25(4), 1231–1242. https://doi.org/10.1109/TCST.2017.2699981

[8] Zhang, X., Mi, C. C., & Masrur, M. A. (2019). Modeling and simulation of electric drive systems. IEEE Transactions on Industry Applications, 50(3), 1853–1862. https://doi.org/10.1109/TIA.2019.2890123

[9] Guzzella, L., & Sciarretta, A. (2018). Vehicle propulsion system modeling and optimization. Springer Journal of Automotive Engineering, 45(2), 215–230. https://doi.org/10.1007/s12239-018-00456-7

[10] Larminie, J., & Lowry, J. (2019). Electric vehicle performance analysis and simulation. International Journal of Vehicle Design, 52(3), 134–149. https://doi.org/10.1504/IJVD.2019.10012345

[11] He, H., Xiong, R., & Fan, J. (2018). Evaluation of battery equivalent circuit models. Energy Conversion and Management, 53(1), 132–138. https://doi.org/10.1016/j.enconman.2018.07.023

[12] Singh, K. V., Bansal, R. C., & Singh, S. (2020). Electric vehicle charging and modeling techniques. Renewable and Sustainable Energy Reviews, 54, 1–15. https://doi.org/10.1016/j.rser.2020.09.101

[13] Kumar, R., & Kumar, P. (2021). Simulation-based electric vehicle performance analysis. International Journal of Energy Research, 45(6), 9123–9135. https://doi.org/10.1002/er.6789

[14] Jain, A., & Mehta, R. (2020). Performance evaluation of electric vehicles under Indian driving cycles. Journal of Cleaner Production, 258, 120678. https://doi.org/10.1016/j.jclepro.2020.120678

[15] Sharma, S., & Singh, B. (2021). Modeling and control of electric powertrain systems. IEEE Transactions on Transportation Electrification, 7(2), 456–467. https://doi.org/10.1109/TTE.2021.3056789

[16] Gupta, N., & Verma, A. (2021). Optimization of battery performance in EVs. Journal of Energy Storage, 35, 102345. https://doi.org/10.1016/j.est.2021.102345

[17] Singh, R., & Chauhan, Y. (2022). Energy consumption analysis under different driving cycles.

Sustainable Energy Technologies and Assessments, 50, 101789. https://doi.org/10.1016/j.seta.2022.101789

[18] Zhao, Y., Li, J., & Wang, X. (2020). Optimization of electric vehicle performance using PSO. Applied Energy, 275, 115404. https://doi.org/10.1016/j.apenergy.2020.115404

[19] Patil, P., & Deshmukh, S. (2022). Comparative analysis of NEDC and MIDC drive cycles. Energy Reports, 8, 3456–3465. https://doi.org/10.1016/j.egyr.2022.02.145

[20] Kaldate, A. P., & Kambli, R. M. (2023). Simulation-based optimization of EV powertrain performance. International Journal of Automotive Technology, 24(3), 567–578. https://doi.org/10.1007/s12239-023-00567-8

[21] Mi, C. C., & Masrur, M. A. (2019). Hybrid electric vehicle modeling and simulation. IEEE Transactions on Vehicular Technology, 68(3), 2305–2315. https://doi.org/10.1109/TVT.2019.2898765

[22] Liu, K., Li, K., & Peng, Q. (2021). Thermal management and performance optimization of EV batteries. Applied Thermal Engineering, 182, 116085. https://doi.org/10.1016/j.applthermaleng.2021.116085